

Short Communication

Effects of Microelectrochemical Milling Parameters on the Microstructures of Co40CrNiMo

Changfu Zhang^{1,2,*}, Lili Sun^{1,2}, Pixian Zheng^{1,2}, Ruoyun Liang^{1,2}, Kang Yun^{1,2}

¹ School of Mechatronics Engineering, Xi'an Technological University, Xi'an 710021, China

² Shaanxi Key Laboratory of Non-Traditional Machining, Xi'an 710021, China

*E-mail: cfzhang@xatu.edu.cn

Received: 14 September 2019 / Accepted: 20 November 2019 / Published: 10 February 2020

Microparts made of highly elastic alloys are increasingly applied in many industries, including aeronautics and astronautics, precision devices and so on. However, it is difficult to machine these parts with traditional machining technologies. To solve this problem, nanosecond-pulsed microelectrochemical milling technology is applied to machine microparts out of highly elastic alloys. In this paper, the effects of the main process parameters, namely, the machining voltage, the pulse duration, the electrolyte concentration and the feed rate on the machining accuracy are systematically studied, and then microelectrochemical milling experiments for three typical microstructures from a highly elastic alloy of Co40CrNiMo are carried out. The study shows that a rough electrochemical milling coupled with a finish electrochemical milling using proper parameters can be applied to machine microparts from the difficult-to-machine Co40CrNiMo alloy. The experimental results show that within reasonable ranges of these parameters, the machining accuracy of the microstructures from Co40CrNiMo decreases with increasing working voltage, pulse duration and electrolyte concentration but increases with increasing feed rate. This study provides a probable solution for machining microparts from difficult-to-machine highly elastic alloy materials.

Keywords: Highly elastic material; Microelectrochemical milling; Microelectrode; Nanosecond-pulsed power

1. INTRODUCTION

With the development of microelectromechanical systems (MEMS) and nanotechnologies, microparts of highly elastic materials are increasingly applied in the fields of aeronautics and astronautics, ordnance, precision instruments, and so on. Co40CrNiMo is an alloy material with high elasticity, high strength and high hardness, which is commonly used to manufacture important elastic components.

However, it is challenging to machine microparts out of Co40CrNiMo with common

microcutting technologies and some nontraditional machining technologies because most of them are not ideal for machining this kind of micropart without residual stress, recast layers or microcracks. When micromechanical cutting technologies are applied in machining microparts out of Co40CrNiMo, there are some disadvantages, such as cutting difficulty with common tools, residual stress, tool wear and poor accessibility of the tool. Similarly, electrodischarge machining (EDM), ultrasonic machining (USM), electron beam machining (EBM), laser beam machining (LBM) and electrochemical machining (ECM) have been applied in micromachining [1, 2]. However, EDM, EBM and LBM are thermal manufacturing technologies that create heat-affected layers, resulting in microcracks or changes in the material properties. USM is primarily applied for machining brittle materials.

In contrast with the abovementioned technologies, microelectrochemical machining (micro-ECM) appears to be a promising future micromachining process due to its higher machining rate, better precision, and wider range of materials that can be machined [3-5]. It is a heat-free, stress-free and noncontact machining technique that avoids the problem of tool deformation or breakage. With this technology, microstructures of difficult-to-cut alloys can be achieved without generating residual stress or leaving a defective layer to guarantee that the microparts behave reliably [6].

Micro-ECM has demonstrated excellent development potential in micromachining materials because it can remove materials at the ion scale [7-9]. Kim [10, 11] and Park [12] applied micro-ECM milling technology to machine some microstructures in stainless steel utilizing a dilute electrolyte of 0.1 M H₂SO₄. Liu [13] applied a micro-ECM milling by layer process to machine 2D microshapes and 3D complex microstructures. Maurer [14] used micro-ECM with an ultrashort voltage pulse to fabricate microstructures of Hastelloy B-2, which is difficult to machine on a macroscale because of its work-hardening behavior. Jo [15] used micro-ECM to machine reverse-tapered holes and barrel-shaped holes by controlling machining time and pulse parameters. Schuster [5] applied ultrashort pulse micro-ECM technology to realize three-dimensional machining with submicrometer precision. Zemann [16] found that the manufacturing precision of micro-ECM depended extremely on small working gaps through ultrashort voltage pulses with a nanosecond duration. Skoczypiec [6] applied micro-ECM with nanosecond-ranged voltage pulses to machine microparts, while achieving high localization.

From the abovementioned studies, we can conclude that micro-ECM with ultra-short voltage pulses has been applied for machining special materials without any mechanical forces or thermal influences. In this paper, the effects of the main process parameters on the machining accuracy were studied, and comprehensive micro-ECM milling experiments for three typical microstructures with a highly elastic alloy of Co40CrNiMo were carried out. This study provides a probable solution for machining microparts from difficult-to-machine highly elastic alloy materials, and will be helpful when exploring the practical applications of micro-ECM milling technology.

2. EXPERIMENTAL

In this paper, nanosecond-pulsed micro-ECM milling technology is studied to machine the microparts from a difficult-to-machine highly elastic alloy material of Co40CrNiMo. The technology combines the merits of micro-ECM technology and CNC milling technology to manufacture

microparts with a simple microelectrode. In micro-ECM, the movement trajectory of the microelectrode is precisely controlled with CNC technology to realize electrochemical milling of the microstructures.

A micro-ECM milling setup is employed to machine the microstructures out of Co40CrNiMo. The setup is mainly composed of an X-Y-Z multiaxis platform, a motorized spindle, an air-supported flotation platform, a control system, a measuring system, a DC regulated power supply, a nanosecond pulse power supply, an electrolyte circulating system, etc. The X-Y-Z multiaxis platform can move in the X-axis, Y-axis and Z-axis directions with resolutions of 10 nm and speed ranges of 0.1 $\mu\text{m/s}$ ~ 1 mm/s. The motorized spindle can rotate at a speed of 1,000 ~ 60,000 RPMs. The DC regulated power supply is used to prepare the microelectrode with an online machining method, and the nanosecond pulse power supply is used to machine the microparts.

Before the experiments are carried out, the microelectrode is prepared online with an electrochemical etching method to avoid installing errors from an offline prepared microelectrode, as shown in Fig. 1. In this paper, the microelectrode was prepared with a straight, 300 μm diameter tungsten wire. The tungsten wire was clamped into the spindle as the anode, and the cathode was a stainless steel plate premachined with three different-diameter circular holes. The different-diameter segments of the microelectrode were machined by different-diameter circular holes. Both the cathode and the anode were immersed in 2.0 mol/L KOH electrolyte solution. After the DC regulated power supply was turned on, the electrochemical reaction began with the generation of H_2 bubbles escaping from the stainless steel plate. With electrochemical reactions, the tungsten wire was oxidized to WO_4^{2-} ions and dissolved into the electrolyte solution. By controlling the machining parameters (the working voltage, the immersion depth of the tungsten wire, the electrolyte concentration, etc.), each segment of the stepped shaft electrode was machined with the diameter of the corresponding circular hole. After all the segments were machined, the preparation of the stepped shaft electrode was finished. Fig. 2 shows a machined microelectrode with a working section of 10 μm in diameter.

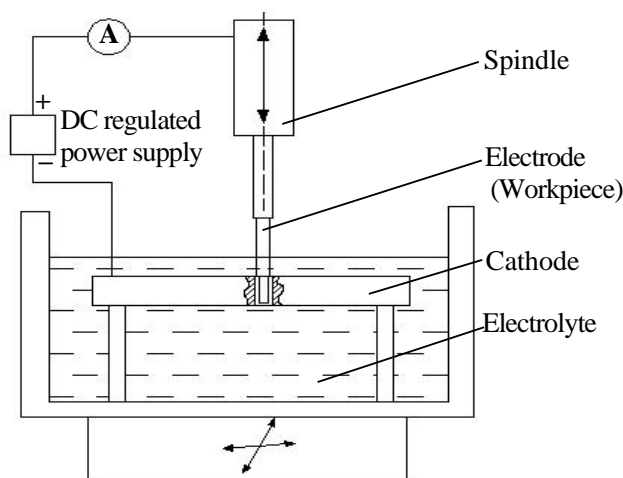


Figure 1. Preparation of the microelectrode online.

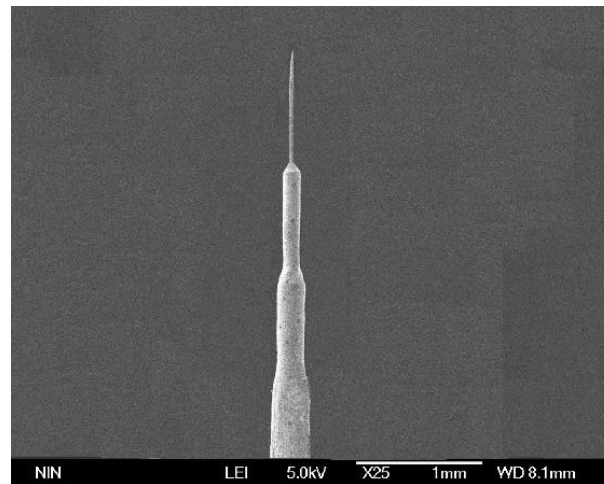


Figure 2. Machined microelectrode.

After the Co40CrNiMo workpiece and the microelectrode were prepared, they were linked with the negative pole and the positive pole of the nanosecond pulse power supply, respectively, and then immersed in a 0.2 mol/L H₂SO₄ electrolyte solution. When the power supply was turned on, the electrochemical reaction began. H⁺ ions near the microelectrode obtained electrons and became H₂ bubbling out of the electrolyte or being carried away by the electrolyte. The metallic atoms of the workpiece lost electrons and became ions entering the electrolyte solution. As the reaction went on, the material of the workpiece near the working section of the microelectrode was continuously etched away, and the microstructure was formed by precisely controlling the movement trajectory of the microelectrode.

To achieve good machining accuracy and efficiency, two processes were employed: rough micro-ECM milling and finish micro-ECM milling. The rough micro-ECM milling was employed to remove the unneeded material rapidly, and the finish micro-ECM milling was used to achieve good machining accuracy.

3. RESULTS AND DISCUSSION

3.1 Relation between the machining accuracy and side-gap

In micro-ECM, the machining gap (including the side gap and the end gap) between the cathode and the anode is a core element that affects the machining accuracy [17]. Within the reasonable ranges of the process parameters, the smaller the machining gap is, the larger the current density is and the higher the machining accuracy is [18]. Therefore, controlling and maintaining a small machining gap is critical to achieving high-accuracy micro-ECM milling [19]. Because the end-gap is difficult to measure directly and precisely, the side-gap is applied to study the machining accuracy of the micro-ECM milling of a highly elastic material of Co40CrNiMo in this paper. A similar method can be seen in [20-22].

The side-gap Δs can be expressed as:

$$\Delta s = (s - D) / 2 \quad (1)$$

where s is the microgroove width (μm), and D is the diameter of the microelectrode (μm).

3.2 Effects of the main process parameters on the machining accuracy in micro-ECM milling of Co40CrNiMo

Since the machining accuracy of micro-ECM milling is affected by multiple parameters (machining voltage, pulse duration, electrolyte concentration, feed rate, etc.), it is necessary to study their effect laws on the machining accuracy of the microparts machined out of Co40CrNiMo. In the following section, the effect laws of the main process parameters, namely, the machining voltage, the pulse duration, the electrolyte concentration and the feed rate on the side gap are studied to evaluate machining accuracy.

3.2.1 Effect of machining voltage on the side-gap

The machining voltage is an important parameter affecting the machining accuracy of micro-ECM milling [23]. A higher machining voltage will result in an increased passage of current, which will increase the amount of material removed [24-26]. To study the effect of the machining voltages on the machining accuracy, six linear microgrooves were electrochemically milled with six different machining voltages on a thin Co40CrNiMo plate of 300 μm thick. Except for the machining voltages, the other main process parameters were kept the same during the machining of the six microgrooves. The machining conditions consisted of six different machining voltages (2.5 V, 3 V, 3.5 V, 4 V, 4.5 V and 5 V), a pulse period of 1.0 μs , a pulse duration of 120 ns, a 0.2 mol/L H_2SO_4 electrolyte solution and a feed rate of 5 $\mu\text{m/s}$.

Then, the average width value of each machined microgroove is calculated by a multipoint measurement-value averaging method. Thus, the side gaps of the six linear microgrooves are obtained with equation (1). With the results, the diagram showing the relationship of “the side-gap - the machining voltage” is obtained, as shown in Fig. 3.

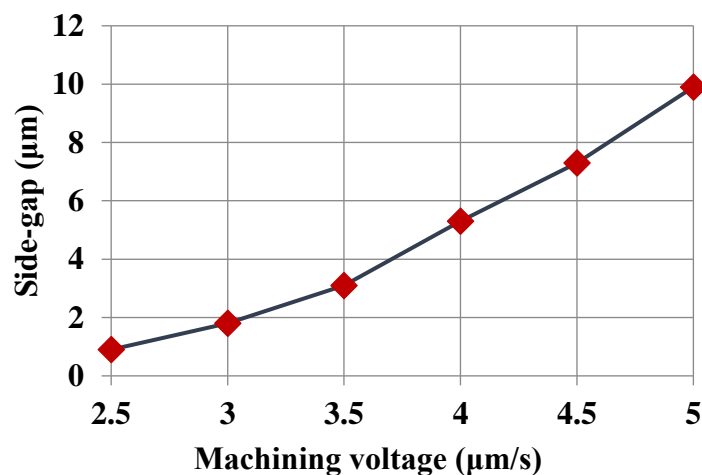


Figure 3. Effect of the machining voltage on the side-gap (pulse period = 1.0 μs , pulse duration = 120 ns, feed rate = 5 $\mu\text{m/s}$ and H_2SO_4 electrolyte concentration = 0.2 mol/L).

As shown in Fig. 3, when the machining voltage increased from 2.5 V to 5 V, the side gaps increased nearly 10 times. According to the diagram, it can be concluded that the larger the voltages are, the larger the side-gaps are, which leads to a decrease of the machining accuracy. Similar results can be seen in [20, 27]. Since the machining current increases as the machining voltage increases,

according to Faraday's law, the larger the machining current is, the larger the corresponding amount of material that is removed. However, a short circuit may occur if the amount of product removed from the micro-ECM is too large and is not flushed away in a timely manner.

Generally, a low machining voltage is often applied in micro-ECM, which helps to reduce the machining gap and stray corrosion and improves the machining localization. However, if the machining voltage is too small, the material removal speed may be lower than the feed rate of the microelectrode, which may result in a short circuit. Thus, the machining voltage is generally 3.0 V ~ 5.0 V to ensure good machining accuracy and stability. Similar results can be seen in [28, 29].

3.2.2 Effect of pulse duration on the side-gap

The pulse duration has an important effect on the electrochemical milling accuracy [30], which can affect the charging time of the electrical double layer (EDL) in a single pulse period [2]. To study the effect of the pulse duration on the machining accuracy of micro-ECM milling, six linear microgrooves are electrochemically milled with six different pulse durations (60 ns, 80 ns, 100 ns, 120 ns, 140 ns and 160 ns) on a thin Co40CrNiMo plate of 300 μm thick. Except for the pulse durations, the other main process parameters are kept the same during the machining of the six microgrooves. The machining conditions consist of a machining voltage of 3 V, a pulse period of 1.0 μs , a 0.2 mol/L H_2SO_4 electrolyte solution and a feed rate of 5 $\mu\text{m/s}$.

Then, the average width value of each microgroove is calculated by the multipoint measurement-value averaging method. Thus, the side gaps of the six linear microgrooves are obtained with equation (1). With the results, the diagram showing the relationship of “the side-gap - the pulse duration” is obtained, as shown in Fig. 4.

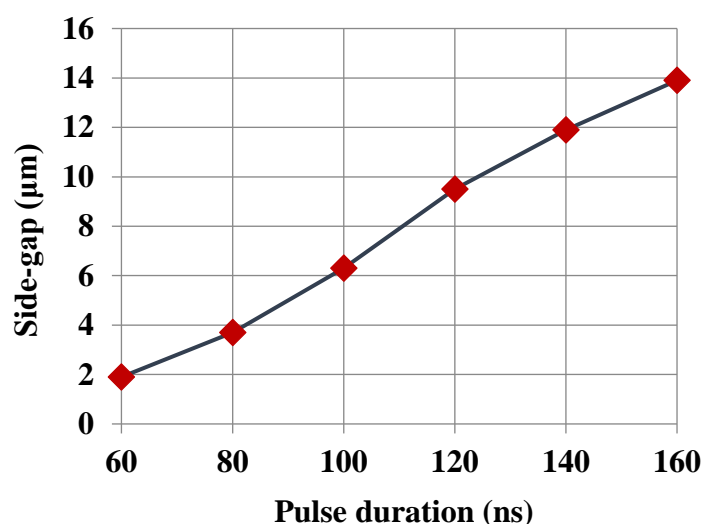


Figure 4. Effect of the pulse duration on the side-gap (machining voltage = 3 V, pulse period = 1.0 μs , H_2SO_4 electrolyte concentration = 0.2 mol/L and feed rate = 5 $\mu\text{m/s}$).

As shown in Fig. 4, the side gap becomes larger as the pulse duration increases. Similar results can be seen in [20, 29]. According to the analysis, when the pulse period is constant and the pulse duration increases, the charging time of the EDL becomes longer, and the machining current becomes larger [31]. According to Faraday's law, the larger the machining current is, the larger the amount of

material removed. Therefore, the amount of lateral material removal in the machining area is inevitably increased, which makes the side-gap increase and the machining accuracy decrease. Generally, a pulse duration is selected to be less than 150 ns to ensure high machining accuracy in micro-ECM. Similar results can be seen in [28, 29, 32, 33].

3.2.3 Effect of electrolyte concentration on the side-gap

In micro-ECM milling, the electrolyte concentration plays an important role in machining accuracy [2]. Many studies have investigated how the electrolyte concentration affects ECM and micro-ECM [34-36]. Changing the electrolyte concentration will cause conductivity changes, which further affect the machining accuracy and rates. To study the effect of the electrolyte concentration on the machining accuracy of micro-ECM milling, five linear microgrooves are electrochemically milled with five different concentrations (0.1 mol/L, 0.2 mol/L, 0.3 mol/L, 0.4 mol/L and 0.5 mol/L) of H_2SO_4 electrolyte solution on a thin Co40CrNiMo plate of 300 μm thick. Except for the electrolyte concentration, the other main process parameters are kept the same during the machining of the five microgrooves. The machining conditions consist of a machining voltage of 3 V, a pulse period of 1.0 μs , a pulse duration of 120 ns and a feed rate of 5 $\mu m/s$.

Then, the average width value of each microgroove is calculated by the multipoint measurement-value averaging method. Thus, the side gaps of the five linear microgrooves are obtained with equation (1). With the results, the diagram showing the relationship of “the side-gap - the electrolyte concentration” is obtained, as shown in Fig. 5.

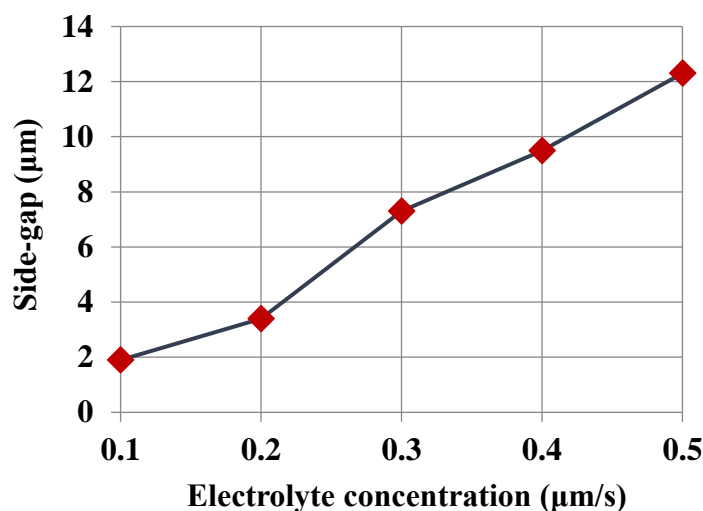


Figure 5. Effect of the electrolyte concentration on the side-gap (machining voltage = 3 V, pulse period = 1.0 μs , pulse duration = 120 ns and feed rate = 5 $\mu m/s$).

Fig. 5 shows that the side-gap increases as the electrolyte concentration increases. A similar result can be seen in [28]. According to the analysis, when the electrolyte concentration increases and the other parameters are constant, the number of charged ions in the electrolyte solution increases, resulting in an increase in the electrical conductivity. The amount of material removed increases accordingly, and the machining locality decreases; thus, the side gap becomes larger, resulting in a

decrease in the machining accuracy. Generally, it is preferable to select a low electrolyte concentration (less than 0.5 mol/L) in micro-ECM milling to ensure machining accuracy and stability. Similar results can be seen in [20, 27]. However, the electrolyte concentration needs to be adjusted when the type of electrolyte changes.

3.2.4 Effect of feed rate on the side-gap

The feed rate is an important process parameter affecting the machining accuracy in micro-ECM milling [37]. To study the effect of the feed rate on the machining accuracy, five linear microgrooves are electrochemically milled with five different feed rates (0.5 $\mu\text{m/s}$, 5 $\mu\text{m/s}$, 10 $\mu\text{m/s}$, 15 $\mu\text{m/s}$ and 20 $\mu\text{m/s}$) on a Co40CrNiMo sheet with a thickness of 300 μm . Except for the feed rates, the other main process parameters are kept the same during the machining of the five microgrooves. The machining conditions consist of a machining voltage of 3 V, a pulse period of 1.0 μs , a pulse duration of 120 ns and a 0.2 mol/L H_2SO_4 electrolyte solution.

Then, the average width value of each microgroove is calculated by the multipoint measurement-value averaging method. Thus, the side gaps of the five linear microgrooves are obtained with equation (1). With the results, the diagram showing the relationship of “the feed rate - the side-gap” can be obtained, as shown in Fig. 6.

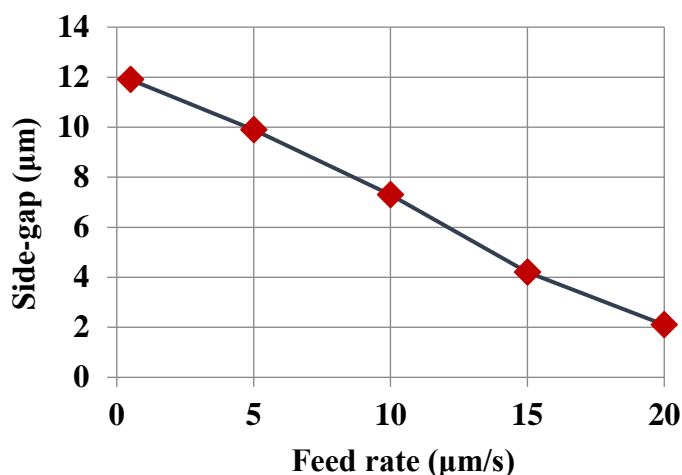


Figure 6. Effect of the feed rate on the side-gap (machining voltage = 3 V, pulse period = 1.0 μs , pulse duration = 120 ns and H_2SO_4 electrolyte concentration = 0.2 mol/L).

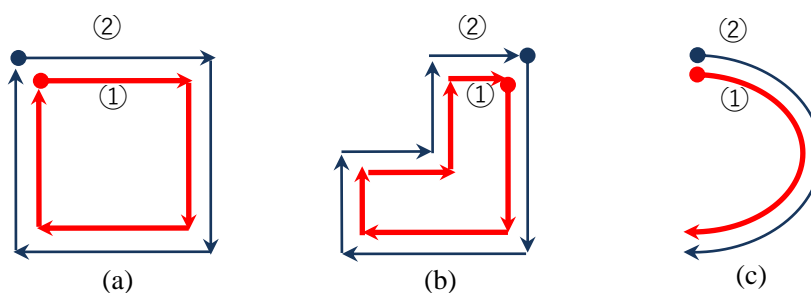
Fig. 6 shows that the side-gap decreases as the feed rate increases. A similar study result can be seen in [27]. According to the analysis, when the feed rate decreases and other parameters remain unchanged, the machining time at a certain point increases, and the removal of material also increases, resulting in an increase in the side gap and a decrease in the machining accuracy. Generally, the feed rate is selected to be 1 $\mu\text{m/s}$ ~ 15 $\mu\text{m/s}$ to achieve good machining accuracy and efficiency. Similar results can be seen in [28, 29].

3.3 Micro-ECM milling of three microstructures out of Co40CrNiMo

To verify and analyze the feasibility of machining microstructures out of a highly elastic alloy of Co40CrNiMo with micro-ECM milling technology, machining experiments for three typical

microstructures (a microsquare hole, a microright-angle groove and a microarc edge) are carried out based on the previous section studying the effects of the main process parameters on machining accuracy.

Two processes, rough micro-ECM milling and finish micro-ECM milling, are employed to machine three kinds of microstructures. A similar method can be seen in [38]. The rough micro-ECM milling is applied to remove the unneeded material rapidly, and the finish micro-ECM milling is used to achieve good machining accuracy. The machining paths of the rough micro-ECM milling and finish micro-ECM milling are shown in Fig. 7. To achieve good results, the optimal process parameters of the rough micro-ECM milling and the finish micro-ECM milling are employed, as shown in Table 1.



① Path of the rough micro-ECM milling. ② Path of the finish micro-ECM milling.

Figure 7. Milling paths of three micro-ECM milling experiments: (a) microsquare hole; (b) microright-angle groove and (c) microarc edge.

Table 1. Optimal process parameters of the rough and finish electrochemical milling processes

Working conditions	Descriptions	
	Rough electrochemical milling	Finish electrochemical milling
Machining voltage /V	4.2	3
Pulse period / μ s	1	1
Pulse duration /ns	150	100
Feed rate / μ m/s	5	8
Diameter of microelectrode / μ m	10	10
Electrolyte (H ₂ SO ₄) /mol/L	0.4	0.2

The three machined microstructures are shown in Fig. 8. It can be seen that these machined microstructures have clear angles or edges. This implies that micro-ECM milling can be applied to machine microstructures from a highly elastic alloy of Co40CrNiMo. To obtain a higher machining speed during the rough micro-ECM milling, some parameter values are increased, namely, the machining voltage, the pulse duration and the electrolyte concentration, while keeping a low feed rate.

To obtain good machining quality in the finish micro-ECM milling, a higher feed rate was utilized with some decreased parameter values, namely, the machining voltage, the pulse duration and the electrolyte concentration. With these two processes, the three microstructures are successfully machined.

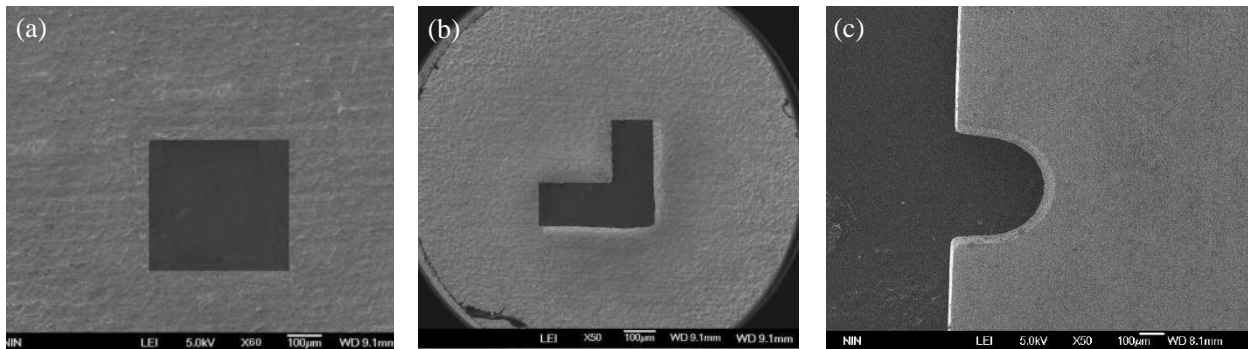


Figure 8. Three microstructures machined with micro-ECM milling: (a) microsquare hole; (b) microright-angle groove and (c) microarc edge.

4. CONCLUSION

In this paper, the effects of the main process parameters, namely, the machining voltage, the pulse duration, the electrolyte concentration and the feed rate on the machining accuracy of micro-ECM milling were studied; furthermore, comprehensive micro-ECM milling experiments for three typical microstructures were carried out with a highly elastic alloy of Co40CrNiMo. The experimental results show that micro-ECM milling technology with a nanosecond pulse power supply could be applied for machining a difficult-to-machine highly elastic alloy of Co40CrNiMo. Rough micro-ECM milling and finish micro-ECM milling with proper parameters were employed to achieve good machining accuracy and efficiency. The study showed that within reasonable ranges of the main process parameters, the machining accuracy of the microstructures with Co40CrNiMo decreases with increasing working voltage, pulse duration and electrolyte concentration but increases with increasing feed rate. This study provides a probable solution for machining microparts from difficult-to-machine highly elastic alloy materials, and will be helpful when exploring the practical applications of micro-ECM milling technology.

ACKNOWLEDGMENTS

This work was financially supported by the National Natural Science Foundation of China (No.51805404), the Projects of Science and Technology Department in Shaanxi Province (No.2014JM2-5072, No.2014SZS20-Z02 and No.2014SZS20-P06) and the Projects of the Department of Education in Shaanxi Province (No.13JS043 and No.17JK0367).

References

1. D.K. Chung, H.S. Shin, M.S. Park, B.H. Kim and C.N. Chu, *Int. J. Precis. Eng. Man.*, 12(2011)371.
2. R. Leese and A. Ivanov, *P. I. Mech. Eng. B - J. Eng.*, 232 (2018) 195.
3. M. Malapati and B. Bhattacharyya, *Mater. Manuf. Process.*, 26(2011)1019.
4. A. Spieser and A. Ivanov, *Int. J. Adv. Manuf. Technol.*, 69(2013)563.
5. R. Schuster, V. Kirchner and P. Allongue, *Science*, 289(2000)98.
6. S. Skoczypiec, *Int. J. Adv. Manuf. Technol.*, 87(2016)177.
7. B. Bhattacharyya, B. Doloi and P.S. Sridhar, *J. Mater. Process. Tech.*, 113(2001)201.
8. K.P. Rajurkar, G. Levy and A. Malshe, *CIRP Ann.*, 55(2006)634.
9. L. Xu, Y. Pan and C. Zhao, *Sci. Rep.*, 6(2016)1.
10. B.H. Kim, S.H. Ryu, D.K. Choi and C.N. Chu, *J. Micromech. Microeng.*, 15(2005)124.
11. B.H. Kim, C.W. Na, Y.S. Lee, D.K. Choi and C.N. Chu, *CIRP Ann.*, 54(2005)191.
12. B.J. Park, B.H. Kim and C.N. Chu, *CIRP Ann.*, 55(2006)197.
13. Y. Liu, D. Zhu and L. Zhu, *Int. J. Adv. Manuf. Technol.*, 60(2012)977.
14. J.J. Maurer, J.J. Mallett, J.L. Hudson, S.E. Fick, T.P. Moffat and G.A. Shaw, *Electrochim. Acta.*, 55(2010)952.
15. C.H. Jo, B.H. Kim and C. N. Chu, *CIRP Ann. - Manuf. Techn.*, 58(2009)181.
16. R. Zemann, F. Bleicher and R. Zisser-Pfeifer, *Arch. Mech. Eng.*, 59(2012)313.
17. Y. Li, Y. Zheng, G. Yang and L. Peng, *Sensors Actuat. A*, 108(2003)144.
18. Z. Zeng, Y. Wang, Z. Wang, D. Shan and X. He, *Precis. Eng.*, 36(2012)500.
19. J. Cai, P. Zhou, R. Kang, K. Shan and D. Guo, *Precis. Eng.*, 41(2015)96
20. H.S. Shin, B.H. Kim and C.N. Chu, *J. Micromech. Microeng.*, 18(2008)075009.
21. V. Rathod, B. Doloi and B. Bhattacharyya, *Int. J. Adv. Manuf. Technol.*, 76(2015)51.
22. X. Qi, X. Fang and D. Zhu, *Int. J. Refract. Met. H.*, 71(2018)307.
23. X. Zhang, N. Qu, H. Li and Z. Xu, *Int. J. Adv. Manuf. Technol.*, 81(2015)1475.
24. D.S. Bilgi, V.K. Jain, R. Shekhar and A.V. Kulkarni, *Int. J. Adv. Manuf. Technol.*, 34(2007)79.
25. A.K.M. De Silva, H.S.J. Altena and J.A. McGeough, *CIRP Ann. - Manuf. Techn.*, 52(2003)165.
26. K. Xu, Y. Zeng, P. Li and D. Zhu, *J. Mater. Process. Tech.*, 222(2015)103.
27. H. He, Y. Zeng and N. Qu, *Precis. Eng.*, 45(2016)285.
28. Y. Liu, Y. Jiang, C. Guo, S. Deng and H. Kong, *Micromachines*, 9(2018)402.
29. S.S. Anasane and B. Bhattacharyya, *Int. J. Adv. Manuf. Technol.* 106(2019)1.
30. W. Natsu and D. Kurahata, *Procedia CIRP*, 6(2013)401.
31. Z.W. Fan, L.W. Hourng and M.Y. Lin, *Int. J. Adv. Manuf. Technol.*, 61(2012) 957.
32. E.S. Lee, S.Y. Back and J.T. Lee, *J. Nanosci. Nanotechnol.*, 9(2009)3424.
33. D. Zhan, L. Han, J. Zhang, Q. He, Z.W. Tian and Z.Q. Tian, *Chem. Soc. Rev.*, 46(2017)1526.
34. B. Bhattacharyya, J. Munda and M. Malapati, *Int. J. Mach. Tool Manu.*, 44(2004)1577.
35. V.K. Jain, S. Kalia, A. Sidpara and V.N. Kulkarni, *Int. J. Adv. Manuf. Technol.*, 61(2012)1175.
36. X. Wu, N. Qu, Y. Zeng, D. Zhu, *Int. J. Adv. Manuf. Technol.*, 69(2013)723.
37. B. Bhattacharyya and J. Munda, *Int. J. Mach. Tool Manu.*, 43(2003)1301.
38. M. Gu, Y. Zeng and L. Meng, *Int. J. Electrochem. Sci.*, 14(2019)414.